First principles calculations of the structural, electronic and vibrational properties of the clathrates $Ba_8Al_{16}Ge_{30}$ and $Ba_8Al_{16}Si_{30}$

Emmanuel N Nenghabi and Charles W Myles

Department of Physics, Texas Tech University, MS 1051, Lubbock, TX 79409, USA

Abstract

We have studied the structural, electronic and vibrational properties of the clathrates $Ba_8Al_{16}Ge_{30}$ and $Ba_8Al_{16}Si_{30}$ using the local density approximation (LDA). The equilibrium structures that we have obtained for these materials show that the Si-containing compound $Ba_8Al_{16}Si_{30}$ is energetically more stable than its Ge counterpart $Ba_8Al_{16}Ge_{30}$ by -0.38 eV per atom. We also find that $Ba_8Al_{16}Si_{30}$ is a narrow gap semiconductor with an indirect LDA energy band gap of 0.37 eV along the Γ–M high symmetry direction in the Brillouin zone and that $Ba_8Al_{16}Ge_{30}$ is a direct band gap semiconductor with an energy gap of 0.43 eV. We have also calculated the lattice vibrational modes of these materials and have identified the low frequency 'rattler' modes produced by the motion of the Ba atoms that are loosely bound in the cages of the Al–Ge or Si framework. These low lying Ba modes are thought to play a part in reducing the thermal conductivities of these materials.

1. Introduction

The group IV elements Si, Ge and Sn can form novel open-framework, cage like structures called clathrates. In these structures, all cages are strongly bonded, with all atoms in fourfold connected, covalently bonded configuration similar to the fullerene families [1, 2]. These structures have large polyhedral cages that can accommodate foreign impurities or 'guests'. Generally, a clathrate is unstable if its cages are partially filled with guests. These guests are mostly alkali atoms or alkaline earth atoms. There are two common clathrate structural phases, type I and type II. The type I structure is simple cubic, with 46 atoms per unit cell. It has 20-atom cages and 24-atom cages combined in a 2 to 6 ratio. The type II structure is face-centered cubic with 136 atoms per unit cell. It has 20-atom cages and 28-atom cages combined in a ratio 16:8.

The electronic and transport properties of these materials can be tuned both by the choice of guests and the choice of framework constituents [3–8]. The discovery of superconductivity in metal atom doped clathrates [9–12] and the potential of these materials for thermoelectric applications have led to considerable experimental and theoretical research in the search for better thermoelectric materials. The efficiency of a thermoelectric material is given by its figure of merit, $Z = \frac{S^2\sigma}{\kappa}$ where Z is in units of $(K)^{-1}$, S is its Seebeck coefficient, σ is its electrical conductivity and κ is its thermal conductivity. A useful means of describing the thermoelectric efficiency of a material system is by using the dimensionless figure of merit, ZT, where T is the absolute temperature. The higher the ZT value, the better the material is for thermoelectric applications. For bulk thermoelectric materials, a carrier concentration that provides optimum power has been identified [13]. Further optimization is possible by altering the band structure through variation of the framework constituents or by adjusting the carrier concentration. Because the guests are free to rattle in the cages of the clathrates, there is a weak interaction between the guests and the host framework atoms. The rattling frequencies of the guests are therefore localized and can contribute to the lowering of the lattice thermal conductivity by resonantly scattering the acoustic phonon modes from the framework lattice. Theoretical investigations have shown that the host framework modes have many flat phonon dispersion curves. These are responsible for the reduction in the average phonon speed, thus reducing the thermal conductivity [14].

In this paper, we report the results of *ab initio* calculations of the equations of state, crystalline structural parameters, the

electronic band structures and the vibrational spectra for the clathrates $Ba_8Al_{16}Ge_{30}$ and $Ba_8Al_{16}Si_{30}$. These properties are important in material characterization and also vital to obtain an understanding of the thermal conductivity of these materials. It is worthwhile to note that the positions of the Al atoms in the structure affect the energetics of the material. Condron *et al* [15] have found that the Al atoms preferentially fill the 6c sites (3 atoms) before filling the 16i (4 atoms) and 24k sites (9 atoms). We have used this configuration in all our calculations. Considerable experimental [13, 16–18] and theoretical [19, 20] studies have been done on these types of materials with Ga replacing Al. To our knowledge, experimenters have only recently begun studying $Ba_8Al_xGe_{46-x}$ [21] and we are not aware of any published experimental or theoretical investigations of $Ba_8Al_{16}Ge_{30}$ and $Ba_8Al_{16}Si_{30}$.

2. Computational approach

Our calculations are based on the local density approximation (LDA) to density functional theory and we use a plane wave basis with ultrasoft pseudopotentials [22, 23]. The Vienna *ab initio* simulation package (VASP)[1] [25] has been used with the Ceperley–Alder functional [26] to approximate the exchange correlation energy. We optimize the geometry by relaxing the internal coordinates while keeping the lattice constant fixed. We used a $2 \times 2 \times 2$ Monkhorst–Pack k-point grid [27] within the Brillouin zone and a cutoff of energy of 150 eV was employed in all the calculations. Calculations repeated for a $4 \times 4 \times 4$ k-point grid did not produce any appreciable change in the structural, electronic or vibrational properties. The total energy was converged to 10^{-7} eV. This process is repeated for several unit cell volumes until a global minimum energy is found. The resulting energy versus volume curve is fitted with the Birch–Murnaghan equation of state [28][2]. This fitting determines the minimum binding energy E_0 (the binding energy compared to that of free atoms), the corresponding volume V_0 and other parameters. The band structures and total electronic density of states are calculated at the optimized structure, along the high symmetry directions in the Brillouin zone.

The dispersion relations are obtained from the dynamical matrix $D(q)$. A calculation of $D(q)$ requires the computation of second derivatives of the LDA binding energy with respect to atomic displacements. Each atom is given a small finite displacement U_0 (0.02 Å) in the $+U_0$ and $-U_0$ directions and the average force constant is obtained from the second derivative of the energy. Within the harmonic approximation, these forces are proportional to the displacements. Each such small displacement generates a row of force constant matrix elements. We obtain $D(q)$ by taking the Fourier transform of the force constant $3N \times 3N$ matrix, where N is the number

Table 1. The parameters of the Birch–Murnaghan equation of state (at $T = 0$ K) obtained from a fit of the LDA energy versus volume curve. E_0 is the minimum binding energy, V_0 is the volume per atom at E_0, a is the lattice constant at E_0, K is the bulk modulus and K' is the pressure derivative of the bulk modulus.

Clathrate	E_0 (eV/atom)	V_0 (Å^3/atom)	a (Å)	K (GPa)	K'
$Ba_8Al_{16}Ge_{30}$	−4.72	23.20	10.78	65.9	2.7
$Ba_8Al_{16}Si_{30}$	−5.10	21.78	10.56	66.6	2.4

of atoms in the unit cell. $D(q)$ is then diagonalized to obtain the zero phonon wavevector vibrational eigenvectors and eigenvalues.

In the second step, for non-zero phonon wavevector, we compute the real space force constant matrix. Only the first, second, and third nearest neighbor pairs of atom matrix elements are included in this calculation. Reference [29] gives the details of this method. Once the force constant matrix is obtained, $D(q)$ and its eigenvalues and eigenvectors are obtained in the usual way. Computer runs were performed on 64 nodes with dual quad-core Intel 5345 processors (2.33 GHz) and 12 GB of memory each. A typical minimization of $4 \times 4 \times 4$ k-point grid needed 51 ionic steps and a total of 160 electronic iterations that took 2 h of CPU time to converge when running on 8 nodes.
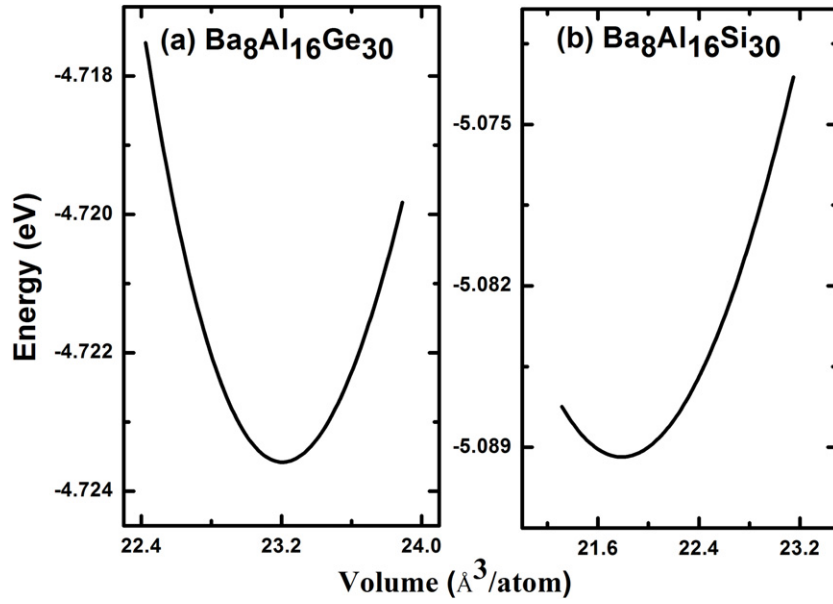
3. Results and discussions

The type I clathrates $Ba_8Al_{16}Ge_{30}$ and $Ba_8Al_{16}Si_{30}$ are simple cubic structures with space group $Pm3n$ (No. 223). The Birch–Murnaghan parameters obtained by optimization of the geometry are: E_0 is the binding energy per atom, V_0 the volume per atom, K the bulk modulus and K' the pressure derivative of the bulk modulus. Our results for these parameters for $Ba_8Al_{16}Ge_{30}$ and $Ba_8Al_{16}Si_{30}$ resulting from the structural optimization are shown in table 1. The equation of state curves (binding energy versus volume) at $T = 0$ K are shown in figure 1. We find that the lattice constant in $Ba_8Al_{16}Si_{30}$ is 10.56 Å and that for $Ba_8Al_{16}Ge_{30}$ is 10.78 Å in as can be seen in table 1. The difference between the two lattice constants is most likely caused by the fact that the size of the Ge atom is larger than the Si atom and thus it has a greater effect on the size of the unit cell.

We have also calculated the total formation energies (E_f) for $Ba_8Al_{16}Ge_{30}$ and $Ba_8Al_{16}Si_{30}$. This quantity determines if it is energetically favorable for a material to form in comparison with solid formed by its constituents (Ba, Al, Si and Ge). This has the form:

$$E_f (Ba_8Al_{16}X_{30}) = E_{Ba_8Al_{16}X_{30}} - 8E_{Ba} - 16E_{Al} - 30E_X$$

where X = (Ge, Si). E_{Ba} is the energy per Ba atom in Ba metal and the definition is similar for the other constituents. We find that the formation energy for $Ba_8Al_{16}Ge_{30}$ is −22.7 eV per unit cell and −20.6 eV per unit cell for $Ba_8Al_{16}Si_{30}$. These results predict that these clathrates are more thermodynamically stable than their isolated bulk constituents and that is energetically favorable for them to form. Our LDA calculations also

---

[1] This program was developed at the Institute für Theoretish Physik of the Technische Universität Wien [24].

[2] The Birch–Murnaghan equation for the energy E as a function of volume V is $E(V) = E_0 + \frac{9}{8}KV_0[(\frac{V_0}{V})^{\frac{2}{3}} - 1]^2\{1 + [\frac{4-K'}{2}][1 - (\frac{V_0}{V})^{\frac{2}{3}}]\}$ where E and E_0 are the energy and minimum energy, V and V_0 is the volume and volume at the minimum energy, K and K' are the bulk modulus and its pressure derivative.

Figure 1. Equations of state (binding energy versus volume) for (a) $Ba_8Al_{16}Ge_{30}$ and (b) $Ba_8Al_{16}Si_{30}$. The LDA-calculated total energy has been fitted to the Birch–Murnaghan equation. Table 1 gives the resulting parameters.
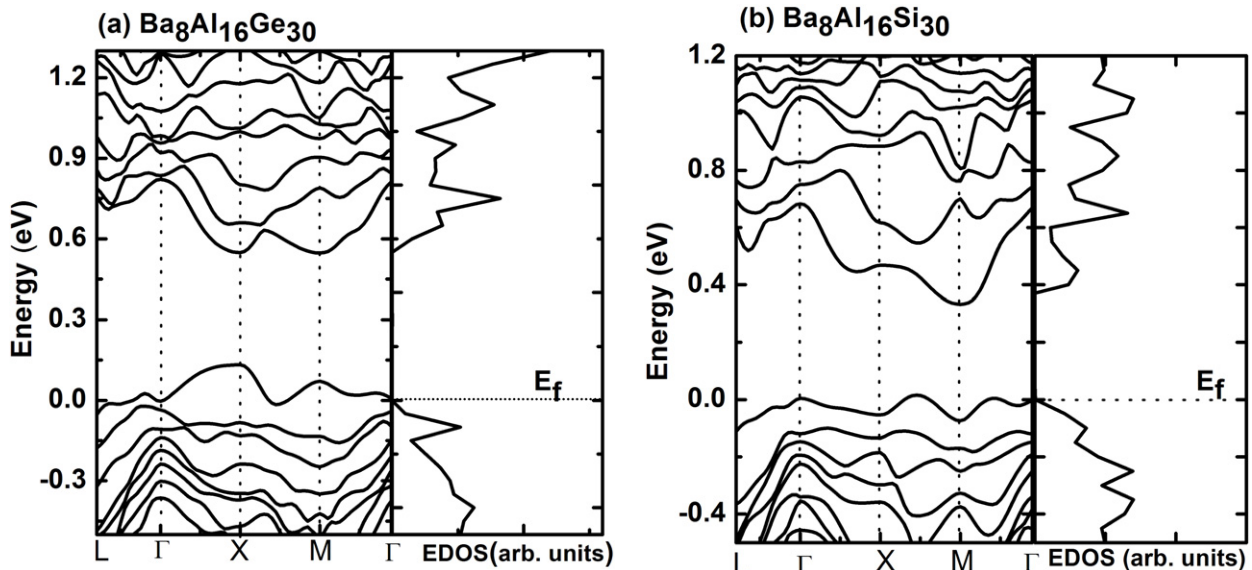
Figure 2. The LDA electronic band structures for (a) $Ba_8Al_{16}Ge_{30}$ and (b) $Ba_8Al_{16}Si_{30}$. Only the region near the band gap is shown. In units of $2\pi/a$, the k points correspond to L $= (1/2, 1/2, 1/2)$, $\Gamma = (0, 0, 0)$, X $= (1/2, 0, 0)$ and M $= (1/2, 1/2, 0)$. The total electronic density of states (EDOS) of each clathrate is also shown. The Fermi level has been set at 0 eV.

predict that $Ba_8Al_{16}Si_{30}$ is thermodynamically more stable than $Ba_8Al_{16}Ge_{30}$ by as much as -0.38 eV per atom.

The calculated bond angles in $Ba_8Al_{16}Ge_{30}$ and $Ba_8Al_{16}Si_{30}$ range from $103.1°$ to $124.2°$ thus deviating from the tetrahedral bond angle of $109.5°$ as is typical in clathrates. The spread in bond angles is similar to results obtained in pristine Ge_{46} and Si_{46} clathrate materials [30, 31].

Starting with the equilibrium structures, calculations of the electronic band structure and the total electronic density of states (EDOS) were carried out for $Ba_8Al_{16}Ge_{30}$ and $Ba_8Al_{16}Si_{30}$. These results are shown in figures 2(a) and (b) respectively. The EDOS are qualitatively similar to each other in the two materials. The Fermi level has been set at 0 eV in

both materials. We find that the valence band maximum and the conduction band minimum are located at the X symmetry point with a direct band gap of 0.43 eV in $Ba_8Al_{16}Ge_{30}$. For $Ba_8Al_{30}Si_{30}$, we find that it is on the Γ–M symmetry line with an indirect energy gap of 0.37 eV. It is well known that the LDA usually underestimates the band gap [30]. For example, the LDA predicts that diamond phase Ge has zero band gap while, experimentally, diamond phase Ge is a semiconductor with an indirect band gap of 0.7 eV. The LDA thus underestimates the band gap in diamond phase Ge by at least 0.7 eV. For this reason, we anticipate that the true band gaps in these materials are larger than those we have calculated. This is consistent with results that have been found for other clathrate materials [19].
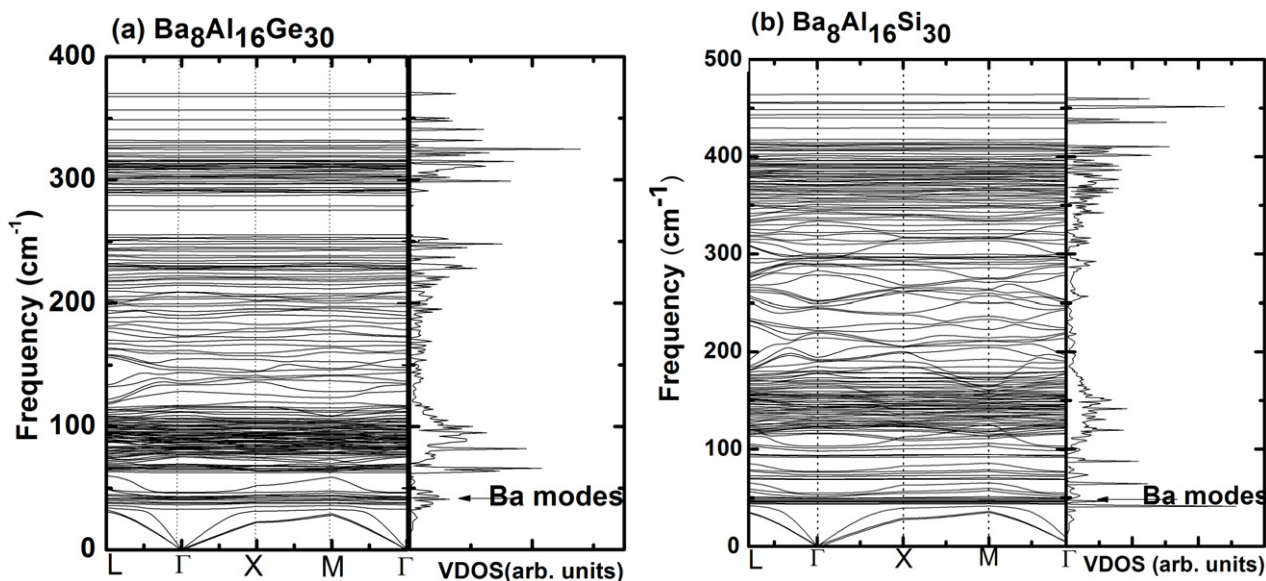
Figure 3. Phonon dispersion relations and vibrational density of states (VDOS) for (a) $Ba_8Al_{16}Ge_{30}$ and (b) $Ba_8Al_{16}Si_{30}$.

By using the Zintl concept [32] to explain the bonding in the $Ba_8Al_{16}Ge_{30}$ and $Ba_8Al_{16}Si_{30}$ clathrates along with our LDA calculations, we predict that both materials are semiconductors. The reasoning for this conclusion is as follows. The Ba atoms donate sixteen electrons to the host so that the valence requirements (octet rule) for the Al atoms on the framework are satisfied. This results in covalently bonded Al–Ge or Al–Si cage structures. Therefore, all framework bonds are saturated, and these materials are semiconductors. On the other hand, the bonds between the Ba atoms and the host framework atoms have an ionic character.

The calculated vibrational dispersion curves and vibrational density of states (VDOS) for $Ba_8Al_{16}Ge_{30}$ and $Ba_8Al_{16}Si_{30}$ are shown in figures 3(a) and (b) respectively. There exist two regions of high vibrational state density in both materials. An eigenvector analysis shows that the first region is due to the flat Ba-related phonon bands appear in the region 35–50 cm^{-1} for both clathrates. These bands cut through the acoustic branches of the framework and display an *avoided crossing* effect. These low rattling modes of the Ba atoms that lie below 50 cm^{-1} should compress the bandwidth of the highly dispersive heat carrying acoustic phonon modes of the host, potentially reducing the lattice thermal conductivity of these clathrates. These low frequency modes are also likely responsible for the bandwidth suppression in $Ba_8Al_{16}Ge_{30}$ and $Ba_8Al_{16}Si_{30}$. The second region of high state density is at the top of the optical bands (above 300 cm^{-1} in figure 3(a) and above 400 cm^{-1} in figure 3(b)). These flat optical modes contribute negligibly to heat transport. For comparison with the present results, phonon spectra for pristine Ge and Si clathrates are discussed in [30] and [31].

As seen in the VDOS portions of figures 3(a) and (b), there is a frequency up-shift by about 100 cm^{-1} in the vibrational spectrum of $Ba_8Al_{16}Si_{30}$ compared to that of $Ba_8Al_{16}Ge_{30}$. The bands also become flatter. This is due to the bond-stretching modes arising from the Si–Si bonds [33]. As can be seen in table 1, the size of the unit cell of $Ba_8Al_{16}Si_{30}$ is smaller than that of $Ba_8Al_{16}Ge_{30}$ because of the size of the Si atom (compared to that of the Ge atom) in the framework. The average Si–Si bond length we find for $Ba_8Al_{16}Si_{30}$ (2.36–2.44 Å) is shorter than we find for $Ba_8Al_{16}Ge_{30}$ (2.43–2.53 Å). These shorter Si–Si bonds increase the stretching force between the Si atoms leading to higher vibrational frequencies.

4. Conclusion

We have used the LDA to study the structural, electronic, and vibrational properties of the clathrates $Ba_8Al_{16}Ge_{30}$ and $Ba_8Al_{16}Si_{30}$. Based on our results for their formation energies, we predict that the formation of both clathrates are energetically favorable. We also find that both materials are semiconductors. Our results predict that $Ba_8Al_{16}Ge_{30}$ has a direct band gap of 0.43 eV and that $Ba_8Al_{16}Si_{30}$ has an indirect band gap of 0.37 eV. The total electronic densities of states for these materials are similar to each other. The phonon spectra of these materials have also been calculated and we find that the low lying Ba 'rattler' vibrational modes lie below 50 cm^{-1}. We also find an up-shift in frequencies in $Ba_8Al_{16}Si_{30}$ by 100 cm^{-1} when compared to $Ba_8Al_{16}Ge_{30}$. This is due to shorter stronger Si–Si bonds that increase the stretching force between the atoms.

Acknowledgment

References

[1] Kasper J, Hagenmuller P, Pouchard M and Cros C 1965 *Science* **150** 1713
[2] Cros C, Pouchard M and Hagenmuller P 1965 *J. Solid State Chem.* **2** 570

[3] Nolas G S, Ward J M, Gryko J, Qiu L and White M A 2001 *Phys. Rev.* B **64** 153201

[4] Nolas G S, Weakley T J R, Cohn J L and Sharma R 2000 *Phys. Rev.* B **61** 3845

[5] Nolas G S, Cohn J L, Slack G A and Schujman S B 1998 *Appl. Phys. Lett.* **73** 178

[6] Cohn J L, Nolas G S, Fessatidis V, Metcalf T H and Slack G A 1999 *Phys. Rev. Lett.* **82** 779

[7] Myles C W, Dong J and Sankey O F 2001 *Phys. Rev.* B **64** 165202

[8] Biswas K and Myles C W 2007 *Phys. Rev.* B **75** 245205

[9] Kawaji H, Horie H, Yamanaka S and Ishikawa M 1995 *Phys. Rev. Lett.* **74** 1427

[10] Yamanaka S, Horie H, Kawaji H and Ishikawa M 1996 *Eur. J. Solid State Inorg. Chem.* **32** 799

[11] Kawaji H, Iwai K, Yamanaka S and Ishikawa M 1996 *Solid State Commun.* **100** 393

[12] Yamanaka S, Enishi E, Fukuoka H and Yasukawa M 2000 *Inorg. Chem.* **39** 56

[13] Blake N P, Mollnitz L, Kresse G and Metiu H 1999 *J. Chem. Phys.* **111** 3133

[14] Dong J, Sankey O F, Ramachandran G K and McMillan P F 2000 *J. Appl. Phys.* **87** 7726

[15] Condron C L, Martin J, Nolas G S, Piccoli P M B, Schultz A J and Kauzlarich S M 2006 *Inorg. Chem.* **45** 9381–6

Condron C L, Porter R, Guo T and Kauzlarich S M 2005 *Inorg. Chem.* **44** 9185–91

Condron C L and Kauzlarich S M 2006 *Inorg. Chem.* **46** 2556–62

[16] Qiu L, Swainson I P, Nolas G S and White M A 2004 *Phys. Rev.* B **70** 035208

[17] Sales B C, Chakoumakos B C, Jin R, Thompson J R and Mandrus D 2001 *Phys. Rev.* B **63** 245113

[18] Kuznetsov V L, Kuznetsova L A, Kaliazin A E and Rowe D M 2000 *J. Appl. Phys.* **87** 7871

[19] Blake N P, Latturner S, Bryan J D, Stucky G D and Metiu H 2001 *J. Chem. Phys.* **115** 8060

[20] Blake N P, Bryan D, Latturner S, Molltnitz L, Stucky G D and Metiu H 2001 *J. Chem. Phys.* **114** 10063

[21] Gou W, Chi J, Li Y, Goruganti V and Ross J H 2007 Experimental study of $Ba_8Al_xGe_{46-x}$ clathrates by NMR and other techniques *Texas Section of the APS March Mtg (Oct. 2007)*

[22] Vanderbilt D 1990 *Phys. Rev.* B **41** 7892

Laasonen K, Car R, Lee C and Vanderbilt D 1991 *Phys. Rev.* B **43** 796

[23] Kresse G and Hafner J 1994 *J. Phys.: Condens. Matter* **6** 8245

Kresse G and Hafner J 1993 *Phys. Rev.* B **48** 13115

[24] Kresse G and Furthmuller J 1996 *Comput. Mater. Sci.* **6** 15

[25] Kresse G and Hafner J 1993 *Phys. Rev.* B **47** 558

Kresse G and Hafner J 1996 *Phys. Rev.* B **55** 11169

[26] Ceperley D M and Alder B J 1980 *Phys. Rev. Lett.* **45** 566

[27] Monkhorst H J and Pack J D 1976 *Phys. Rev.* B **13** 5188

[28] Birch F 1952 *J. Geophys. Res.* **57** 227

[29] Dong J, Sankey O F and Kern G 1999 *Phys. Rev.* B **60** 950

[30] Dong J and Sankey O F 1999 *J. Phys.: Condens. Matter* **11** 6129–45

[31] Kahn D and Lu J P 1997 *Phys. Rev.* B **56** 13898

[32] Schaffer H 1985 *Annu. Rev. Mater. Sci.* **15** 1

[33] Nolas G S, Kendziora C A, Gryko J, Dong J, Myles C W, Poddar A and Sankey O F 2002 *J. Appl. Phys.* **92** 7225